

TTKK/12.12.1999

73154 TOPICS IN APPLIED MATHEMATICS  
MODELING AND COMPUTER SIMULATION OF MULTIDOMAIN PHYSICAL  
SYSTEMS

PAPER FINISHING DRIVE AND ROLLER MECHANISM

Juha-Matti Kivinen 125104

Ville Järvinen 113418

## 1. INTRODUCTION

Today's trend in papermaking is to improve the surface quality of the paper by coating and calendering processes, where the paper web is thermomechanically modified in roll nips [Smook 1997]. The production problems arise from the fact that the running speeds of the base paper machine may reach levels 1400...1800 m/min. Especially coating and calendering (figure 1) are very speed-sensitive processes so that at higher speeds the rolls in nip contact may vibrate causing both maintenance and quality problems.

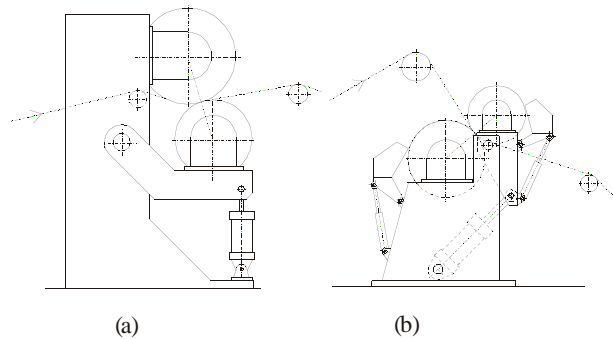


Figure 1. Typical nip units used in a) calendering and b) coating processes [Kivinen et al 1999].

In most cases the roll covers might be an important element in the vibration. Observations have shown that depending on the configuration of the roll mechanism the relative motion of the rolls may exist in tangential or normal direction with respect to the nip line. The frequencies match with the gear meshes of the roll drives but some self-excited vibrations occur also at the eigenfrequencies of the rolls.

## 2. NIP UNIT MECHANISMS

Nip units typically contain two main mechanisms, the loading and the drive mechanisms. The configuration of a typical nip unit is shown below. In this study the drive mechanism is the working hypothesis.

The components of the drive mechanism are electrical motors, gearboxes, universal shafts, couplings and rolls. The speeds of the rolls are usually controlled in such a way that the torque transmitted through the nip will be minimized.

### 3. VIBRATION PROBLEMS IN NIP UNITS

The main task of nip mechanisms is to work in steady-state conditions producing desired line loadings and running speeds. Unfortunately some physical effects modify this static running situation so that a remarkable dynamic component may appear and disturb the surface manipulation in the nip contact area. Based on observations done in European paper mills the rolls undergo dynamic motions in transverse and rotational directions. Generally the cylindrical rolls may vibrate in complicated shell-modes but rolls typically used in nip units have combined modes in first (bending) and second (elliptic deformation) harmonic shell-modes [Hermanski 1995]. Roll drives have also torsionally elastic members in the universal shafts and in the gears where the circumferential variation of the elasticity in the teeth contact may cause a parametric excitation source. In order to reduce the roll vibrations in tangential direction the excitations generated by the gear meshing should be isolated from the rolls by a low-pass filter. In other words: the high-frequency gear excitations are not allowed to enter the rolls and this is arranged by an elastic shaft link. This manner helps also in isolating the torsional disturbances generated by the frequency control of the electrical drives.

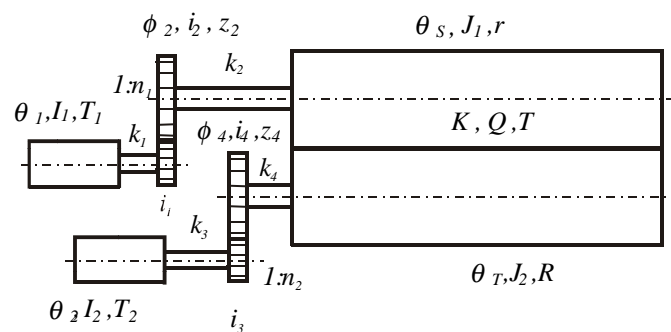


Figure 2. Mass-spring model of the rotating transmission system in calender drives. Parameter  $K$  is the tangential nip stiffness.

From the dynamics point of view this system is composed of concentrated masses connected by elastic shafts.

By using ODE:s the energies for the upper rotors and the first gears ( numbers 1 & 3 ) are

$$\begin{aligned}
 T^* &= \frac{1}{2}I_1\dot{\theta}_1^2 + \frac{1}{2}i_1\dot{\phi}_1^2 & T^* &= \frac{1}{2}I_2\dot{\theta}_2^2 + \frac{1}{2}i_3\dot{\phi}_3^2 \\
 E &= \frac{1}{2}k_1(\theta_1 - \phi_1)^2 & \text{and} & & E &= \frac{1}{2}k_3(\theta_2 - \phi_3)^2 \\
 \mathbf{Q} &= \begin{matrix} T_1 \\ -A_1r_1 \end{matrix} & & & \mathbf{Q} &= \begin{matrix} -T_2 \\ -A_2r_r \end{matrix}
 \end{aligned} \tag{1}$$

and for the rolls and second gears ( numbers 2 & 4 )

$$\begin{aligned}
 T^* &= \frac{1}{2}J_1\dot{\theta}_s^2 + \frac{1}{2}i_2\dot{\phi}_2^2 & T^* &= \frac{1}{2}J_2\dot{\theta}_T^2 + \frac{1}{2}i_4\dot{\phi}_4^2 \\
 E &= \frac{1}{2}k_2(\theta_s - \phi_2)^2 & \text{and} & & E &= \frac{1}{2}k_1(\theta_T - \phi_4)^2 \\
 \mathbf{Q} &= \begin{matrix} -A_1r_2 \\ T - Qr \end{matrix} & & & \mathbf{Q} &= \begin{matrix} -A_2r_4 \\ -T - Qr \end{matrix}
 \end{aligned} \tag{2}$$

with constraints

$$\begin{aligned}
 A_1 &= k(r_1\phi_1 + r_2\phi_2) \\
 A_2 &= k(r_4\phi_4 + r_3\phi_3) \\
 Q &= K(r\theta_s + R\theta_T) \\
 r_1\phi_1 + r_2\phi_2 &= 0 \\
 r_4\phi_4 + r_3\phi_3 &= 0
 \end{aligned} \tag{3}$$

We choose the angular positions of the rolls, drives and gears and get a six degrees of freedom system model for dynamic testing. The system equations are (ODE)

$$\begin{array}{ccccccc}
I_1 & 0 & 0 & 0 & 0 & 0 & \ddot{\theta}_1 \\
0 & i_2 + n_1^2 i_1 & 0 & 0 & 0 & 0 & \ddot{\phi}_2 \\
0 & 0 & J_1 & 0 & 0 & 0 & \ddot{\theta}_s + \dots \\
0 & 0 & 0 & i_4 + n_2^2 i_3 & 0 & 0 & \ddot{\phi}_4 \\
0 & 0 & 0 & 0 & J_2 & 0 & \ddot{\theta}_T \\
0 & 0 & 0 & 0 & 0 & I_2 & \ddot{\theta}_2
\end{array}$$
  

$$\begin{array}{ccccccc}
k_1 & n_1 k_1 & 0 & 0 & 0 & 0 & \theta_1 \\
n_1 k_1 & k_2 + n_1^2 k_1 & -k_2 & 0 & 0 & 0 & \phi_2 \\
0 & -k_2 & k_2 + K r^2 & 0 & K R r & 0 & \theta_s \\
0 & 0 & 0 & k_4 + n_2^2 k_3 & -k_4 & n_2 k_3 & \phi_4 \\
0 & 0 & K R r & -k_4 & k_4 + K R^2 & 0 & \theta_T \\
0 & 0 & 0 & n_2 k_3 & 0 & k_3 & \theta_2
\end{array}
=
\begin{array}{l}
T_1 + \frac{k_1}{r_1} U_0 \sin(z_2 \dot{\phi}_2 t) \\
-\frac{k_1}{r_1} U_0 \sin(z_2 \dot{\phi}_2 t) \\
T \\
\frac{k_3}{r_3} U_0 \sin(z_4 \dot{\phi}_4 t) \\
-T \\
-T_2 - \frac{k_3}{r_3} U_0 \sin(z_4 \dot{\phi}_4 t)
\end{array}$$

(4)

Displacement-controlled loads  $U = U_0 \sin(z_i \dot{\phi}_i t)$ , where  $i = 2, 4$ , represent harmonic variations in the teeth contact. The most interesting question is how the tangential nip force  $Q$  behaves during the vibration motion. One the main sources to cause roll cover damages relates to this tangential force  $Q$ , which is defined  $Q = K(\theta_s r + \theta_T R)$ .

### DAE-FORMULATING

When introducing DAE-formulating, the electric circuits (DC-motors) have been added (Figure 3). The kinetic co-energy and potential energy are

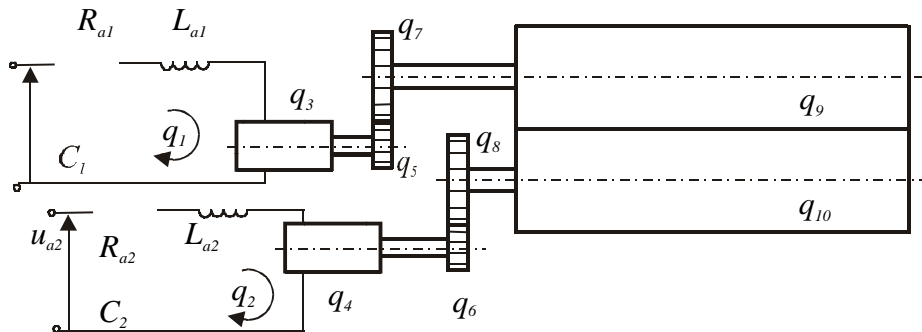


Figure 3. Model for DAE-modeling. Springs and inertia terms introduced in Fig. 2.

$$T^* = \frac{1}{2}L_1\dot{q}_1^2 + \frac{1}{2}I_1\dot{q}_3^2 + \frac{1}{2}i_1\dot{q}_5^2 + \frac{1}{2}i_2\dot{q}_7^2 + \frac{1}{2}J_1\dot{q}_9^2 + \frac{1}{2}L_2\dot{q}_2^2 + \frac{1}{2}I_2\dot{q}_4^2 + \frac{1}{2}i_3\dot{q}_6^2 + \frac{1}{2}i_4\dot{q}_8^2 + \frac{1}{2}J_2\dot{q}_{10}^2 \quad (5)$$

and

$$V = \frac{1}{2}k_1(q_3 - q_5)^2 + \frac{1}{2}k_2(q_7 - q_9)^2 + \frac{1}{2}k_3(q_6 - q_4)^2 + \frac{1}{2}k_4(q_8 - q_{10})^2 + \frac{1}{2}K(q_9 - q_{10})^2 \quad (6)$$

, respectively. The dissipation is

$$D = \frac{1}{2}R_{A1}\dot{q}_1^2 + \frac{1}{2}R_{A2}\dot{q}_2^2 + \frac{1}{2}B\dot{q}_9^2 \quad (7)$$

The kinematic constraints are

$$\begin{aligned} \phi_1 &= q_5 - n_1q_7 = 0 \\ \phi_2 &= q_6 - n_2q_8 = 0 \\ \phi_3 &= q_9 - \frac{R}{r}q_{10} = 0 \end{aligned} \quad (8)$$

Applying the eq. 3.28 from [Layton 1998]

$$\begin{aligned} L_{A1}\dot{f}_1 + R_{A1}f_1 &= U_{A1} - C_1f_3 \\ L_{A2}\dot{f}_2 + R_{A2}f_2 &= U_{A2} - C_2f_4 \\ I_1\dot{f}_3 &= C_1f_1 - k_1(q_3 - q_5) \\ I_2\dot{f}_4 &= C_2f_2 + k_3(q_6 - q_4) \\ i_1\dot{f}_5 - k_1(q_3 - q_5) + \kappa_1 &= 0 \\ i_3\dot{f}_6 + k_3(q_6 - q_4) + \kappa_2 &= 0 \\ i_2\dot{f}_7 + k_2(q_7 - q_9) - n_1\kappa_1 &= 0 \\ i_4\dot{f}_8 + k_4(q_8 - q_{10}) - n_2\kappa_2 &= 0 \\ J_1\dot{f}_9 - k_2(q_7 - q_9) + K(q_9 - q_{10}) + Bf_9 + \kappa_3 &= 0 \\ J_2\dot{f}_{10} - k_4(q_8 - q_{10}) - K(q_9 - q_{10}) - R/r^*\kappa_3 &= 0 \end{aligned} \quad (9)$$

where

$$\begin{aligned}
\dot{q}_1 &= f_1 \\
\dot{q}_2 &= f_2 \\
\dot{q}_3 &= f_3 \\
\dot{q}_4 &= f_4 \\
\dot{q}_5 &= f_5 \\
\dot{q}_6 &= f_6 \\
\dot{q}_7 &= f_7 \\
\dot{q}_8 &= f_8 \\
\dot{q}_9 &= f_9 \\
\dot{q}_{10} &= f_{10}
\end{aligned}
\tag{10}$$

#### 4. NUMERICAL RESULTS OF THE DAE -MODEL

The simulations were carried out by Dynast-solver. The results are transferred from Dynast to Mathcad™ and all the displacements and their derivatives have been plotted as figures 4 to 13. Simulation time for DAE is 6 s. The most difficult task to model this roll mechanism is to find out the real electrical quantities. While calculating with DAE –model the spring ratio  $K$  and parametric excitation have been neglected. Also the controllers for the electrical actuators must be added when a real system is modeled. For the simplicity our model does not include any controllers.

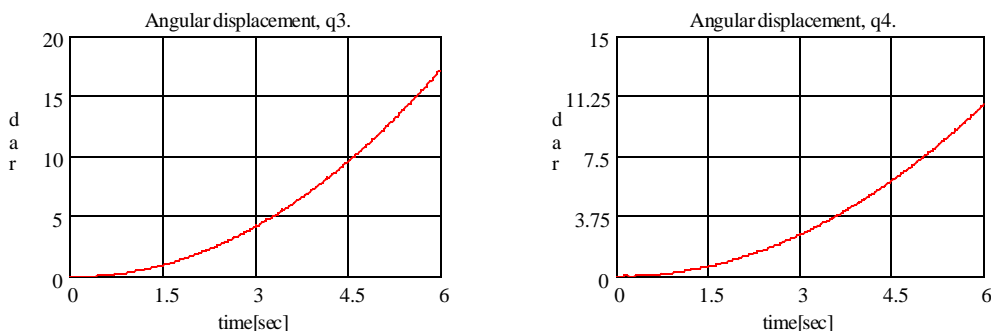


Figure 4. Rolls. Variation of angular displacements of electrical motors with respect to time.

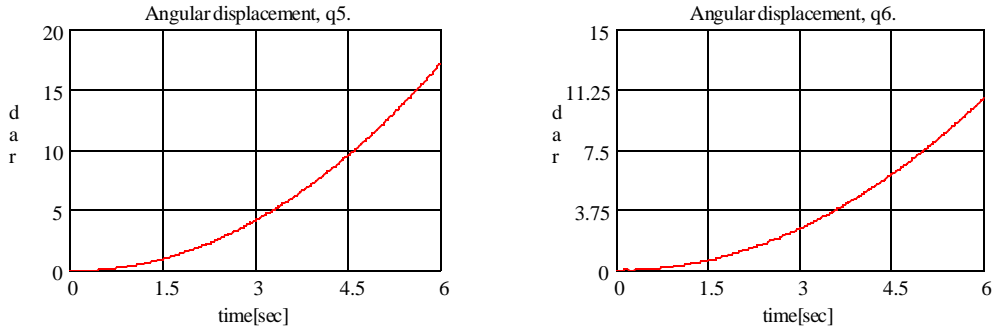


Figure 5. Variation of smaller gears angular displacements with respect to time.

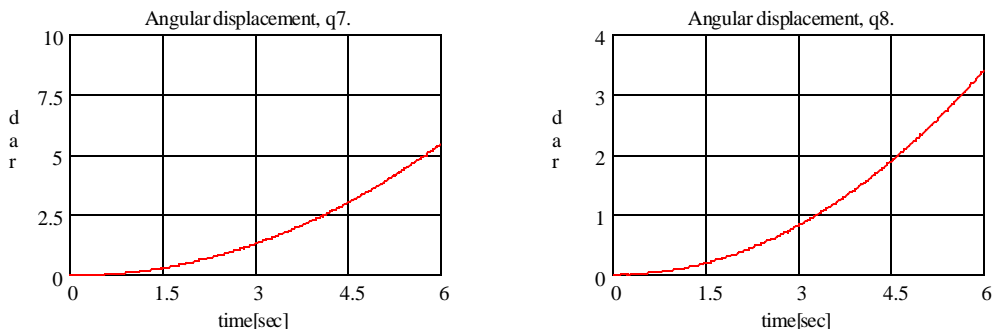


Figure 6. Variation of larger gears angular displacements with respect to time.

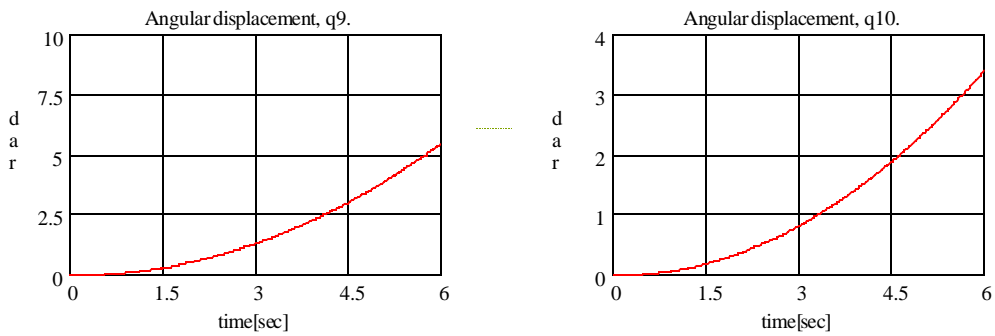


Figure 7. Rolls. Variation of angular displacements with respect to time.

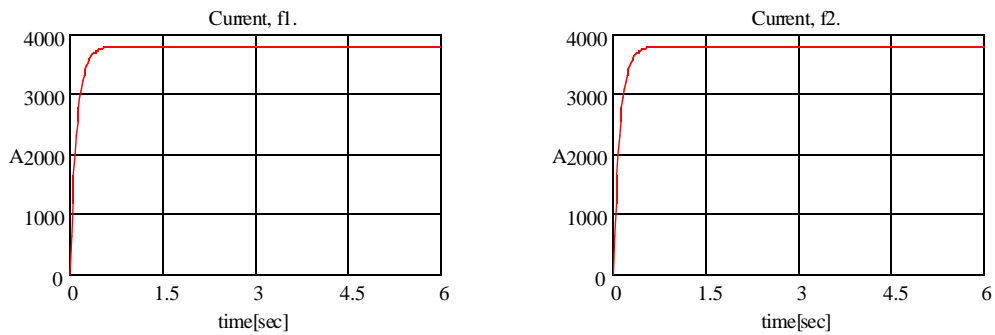


Figure 8. Currents. Variation of  $f_1$  and  $f_2$  with respect to time.

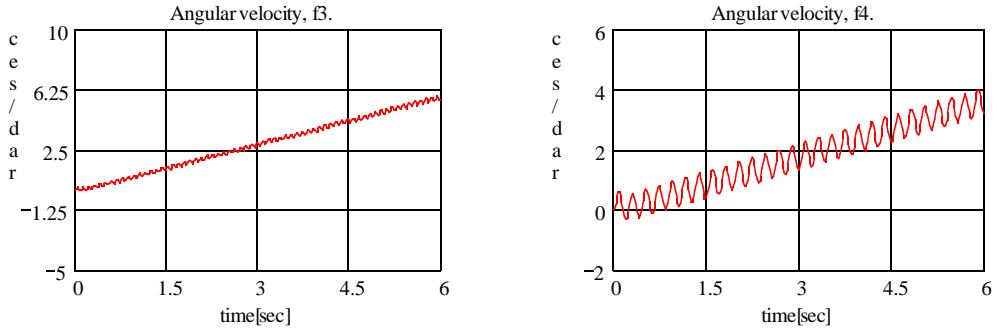


Figure 9. Variations of motor angular velocities  $f_3$  and  $f_4$  with respect to time.

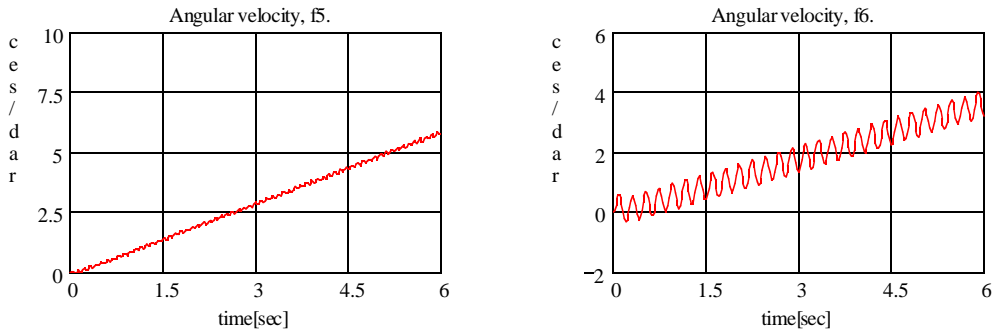


Figure 10. Variations of smaller gear angular velocities  $f_5$  and  $f_6$  with respect to time.

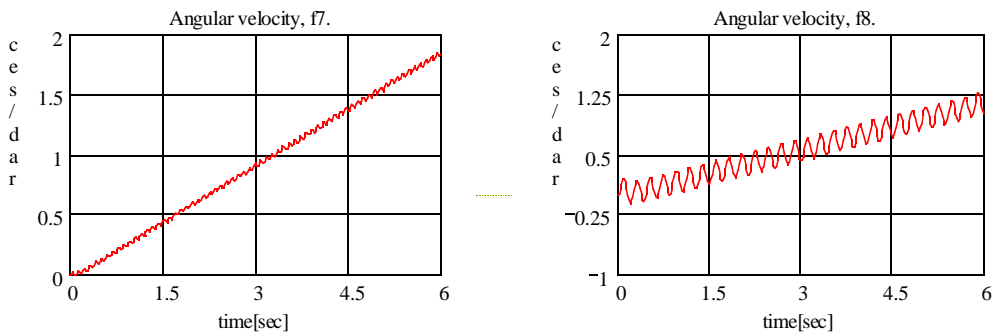


Figure 10. Variations of larger gear angular velocities  $f_7$  and  $f_8$  with respect to time.

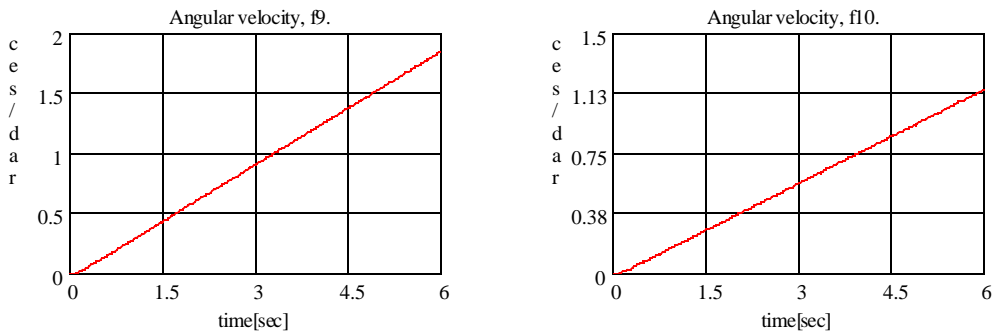


Figure 11. Rolls. Variations of angular velocities  $f_9$  and  $f_{10}$  with respect to time.

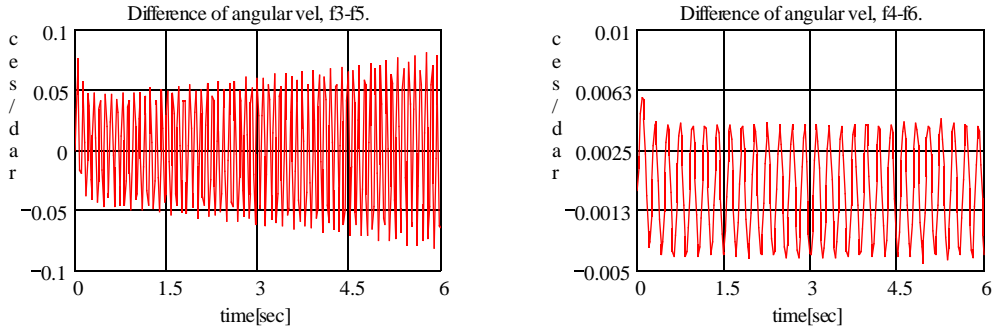


Figure 12. Torsional vibrations in motor shafts. Difference of upper and lower motor shafts angular velocities  $\dot{z}_{mu} = f_3 - f_5$  and  $\dot{z}_{lu} = f_4 - f_6$  during the simulation period, respectively.

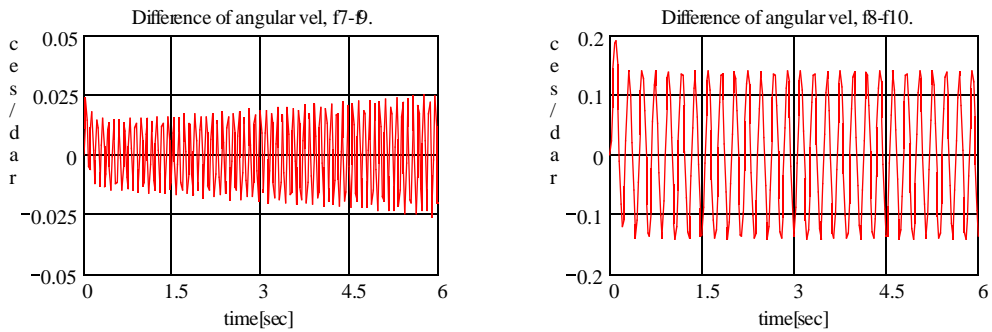


Figure 13. Torsional vibrations in universal shafts. Difference of upper and lower roll shafts angular velocities  $\dot{z}_{ur} = f_7 - f_9$  and  $\dot{z}_{lr} = f_8 - f_{10}$  during the simulation period, respectively.

## APPENDIX 1

### Dynast code:

: File LAYTON2 Date 21/12/1999 Time 08:42:22  
:73154, Topics in Applied Mathematics, EXERCISE

:=====

\*SYSTEM;

: mechanical parameters and functions

i1=0.083; i2=0.11; i3=1.33; i4=i2;  
J1=8500; J2=11000; I1=16.3; I2=I1;  
z\_small=32; z\_large=101;  
r\_small=0.048; r\_large=0.15;  
n1=z\_large/z\_small; n2=n1;  
k1=1.5e5; k2=1.5e6; k3=1.5e6; k4=1.5e5;  
E=5e8; h=0.01; w=7.42; q=150000;  
r=0.42; RR=0.675;  
beta=0.5\*(1/r + 1/r);  
a=(4/3)\*E\*(w/(h\*sqrt(beta)));  
K=0;:(3/2)\*w\*(a\*\*(2/3))\*((q\*w)\*\*(1/3));  
u=(q\*w/a)\*\*(2/3);  
T=244; T1=39/0.7; T2=39/0.7; z2=101; z4=101;  
U0=1e-5; r1=0.3; r3=0.3;

:inertia moments of gear-wheels  
:inertia moments of rolls (J) and armatures (I)  
:number of cogs of gear-wheels  
:radius of gear-wheels  
:gear ratios  
:system stiffnesses  
:numerical constants  
:radius of rolls  
:numerical constant  
:numerical constant  
:tangential stiffness in roll-nip

```

:electrical parameters
ua1=380;      ua2=380;      :armature supply voltages [V]
c1=0.2;      c2= 0.2;      :machine constants [Vs/rad]
ra1=0.1;     ra2=0.1;     :armature resistances [ohm]
La1=10.65e-3; La2=10.65e-3; :armature inductances [H]

```

```

===== equations of motion=====

```

```

SYSVAR q1,q2,q3,q4,q5,q6,q7,q8,q9,q10,
f1,f2,f3,f4,f5,f6,f7,f8,f9,f10,kappa1,kappa2,kappa3;

```

```

:----- d/dt *qi = fi ---

```

```

0 = VD.q1 - f1;
0 = VD.q2 - f2;
0 = VD.q3 - f3;
0 = VD.q4 - f4;
0 = VD.q5 - f5;
0 = VD.q6 - f6;
0 = VD.q7 - f7;
0 = VD.q8 - f8;
0 = VD.q9 - f9;
0 = VD.q10 - f10;

```

```

:-----

```

```

B = 12;                                :damping factor between the rolls

```

```

0 = -VD.f1+ua1/La1-(c1*f3)/La1-(ra1*f1)/La1;
0 = -VD.f2+ua2/La2-(c2*f4)/La2-(ra2*f2)/La2;
0 = -VD.f3+(1/II1)*(c1*f1-k1*(q3-q5));
0 = -VD.f4+(1/II2)*(c2*f2+k3*(q6-q4));
0 = -VD.f5+(1/I1)*(k1*(q3-q5)-kappa1);
0 = -VD.f6+(1/I3)*(-k3*(q6-q4)-kappa2);
0 = -VD.f7+(1/I2)*(-k2*(q7-q9)+n1*kappa1);
0 = -VD.f8+(1/I4)*(-k4*(q8-q10)+n2*kappa2);
0 = -VD.f9+(1/J1)*(k2*(q7-q9)-K*(q9-q10)-B*f9-kappa3);
0 = -VD.f10+(1/J2)*(k4*(q8-q10)+K*(q9-q10)+(r/RR)*kappa3);

```

```

:-----the kinematic constraints-----

```

```

0 = q5-n1*q7;                            :kappa1
0 = q6-n2*q8;                            :kappa2
0 = q9 - (RR/r)*q10;                    :kappa3

```

```

=====

```

```

*TR;
TR 0 6;PRINT (300)
f9,f10;
RUN; *END;

```

## REFERENCES

Cotsaftis, M., Keskinen, E.K., Yuan, L., Vuoristo T., “Effect of Polymer Rheology on Nip Oscillation Dynamics in Covered Roll System”. ASME Materials and Mechanics Conference, Blacksburg, 1999.

Hermanski, M., “Barringbildung am Glättkalander einer Papiermaschine”, *Das Papier*, Heft 9., 1995, pp. 581-590.

Johnson, K.L., “Contact Mechanics”, Cambridge University Press, 1985.

Keskinen, E.K., Kivinen, J.-M. and Launis, S., “Dynamic Analysis of Roll Nip Mechanisms in Papermaking Systems”, Proceedings of the 10th European Simulation Symposium, Ed. Bargiela, A. and Kerckhoffs, E., SCS, Nottingham, 1998, pp. 474-476.

Kivinen, J.-M., Keskinen, E., Järvenpää, V.-M., Cotsaftis, M. and Vikman, K., “A Dynamically Stable Nip Loading Mechanism for Paper Finishing Systems”, Proceedings of the 10th World Congress on The Theory of Machines and Mechanism, Volume 4, Oulu, 1999, pp, 1353-1360.

Layton, R.L., “Principles of Analytical System Dynamics”, Springer-Verlag, New York, 1998.

Smook, G.A., “Handbook for Pulp and Paper Technologists”. Angus Wilde Publ., Vancouver, 1997.